



University  
of Glasgow

Maneuski, D. et al. (2012) Imaging and spectroscopic performance studies of pixellated CdTe Timepix detector. *Journal of Instrumentation*, 7 (1). C01038. ISSN 1748-0221

Copyright © 2012 IOP Publishing Ltd and SISSA

A copy can be downloaded for personal non-commercial research or study, without prior permission or charge

Content must not be changed in any way or reproduced in any format or medium without the formal permission of the copyright holder(s)

When referring to this work, full bibliographic details must be given

<http://eprints.gla.ac.uk/99280>

Deposited on: 11 November 2014

Enlighten – Research publications by members of the University of Glasgow\_  
<http://eprints.gla.ac.uk>

## Imaging and spectroscopic performance studies of pixellated CdTe Timepix detector

This content has been downloaded from IOPscience. Please scroll down to see the full text.

2012 JINST 7 C01038

(<http://iopscience.iop.org/1748-0221/7/01/C01038>)

View [the table of contents for this issue](#), or go to the [journal homepage](#) for more

Download details:

IP Address: 130.209.6.42

This content was downloaded on 11/11/2014 at 14:57

Please note that [terms and conditions apply](#).

THE 9<sup>th</sup> INTERNATIONAL CONFERENCE ON POSITION SENSITIVE DETECTORS,  
12–16 SEPTEMBER 2011,  
ABERYSTWYTH, U.K.

## Imaging and spectroscopic performance studies of pixellated CdTe Timepix detector

D. Maneuski,<sup>a,1</sup> V. Astromskas,<sup>a</sup> E. Fröjdh,<sup>b</sup> C. Fröjdh,<sup>b</sup> E.N. Gimenez,<sup>c</sup> J. Marchal,<sup>c</sup>  
V. O'Shea,<sup>a</sup> G. Stewart,<sup>a</sup> N. Tartoni,<sup>c</sup> H. Wilhelm,<sup>c</sup> K. Wraight<sup>a</sup> and R.M. Zain<sup>a</sup>

<sup>a</sup>*School of Physics and Astronomy, University of Glasgow,  
G12 8QQ, United Kingdom*

<sup>b</sup>*Mid Sweden University,  
Holmgatan 10, 85170, Sundsvall, Sweden*

<sup>c</sup>*Diamond Light Source Ltd.,  
Didcot, Oxfordshire, OX11 0DE, United Kingdom*

E-mail: [dima.maneuski@glasgow.ac.uk](mailto:dima.maneuski@glasgow.ac.uk)

**ABSTRACT:** In this work the results on imaging and spectroscopic performances of  $14 \times 14 \times 1$  mm CdTe detectors with  $55 \times 55 \mu\text{m}$  and  $110 \times 110 \mu\text{m}$  pixel pitch bump-bonded to a Timepix chip are presented. The performance of the  $110 \times 110 \mu\text{m}$  pixel detector was evaluated at the extreme conditions beam line I15 of the Diamond Light Source. The energy of X-rays was set between 25 and 77 keV. The beam was collimated through the edge slits to  $20 \mu\text{m}$  FWHM incident in the middle of the pixel. The detector was operated in the time-over-threshold mode, allowing direct energy measurement. Energy in the neighbouring pixels was summed for spectra reconstruction. Energy resolution at 77 keV was found to be  $\Delta E/E = 3.9\%$ .

Comparative imaging and energy resolution studies were carried out between two pixel size detectors with a fluorescence target X-ray tube and radioactive sources. The  $110 \times 110 \mu\text{m}$  pixel detector exhibited systematically better energy resolution in comparison to  $55 \times 55 \mu\text{m}$ . An imaging performance of  $55 \times 55 \mu\text{m}$  pixellated CdTe detector was assessed using the Modulation Transfer Function (MTF) technique and compared to the larger pixel. A considerable degradation in MTF was observed for bias voltages below  $-300$  V. Significant room for improvement of the detector performance was identified both for imaging and spectroscopy and is discussed.

**KEYWORDS:** Gamma detectors (scintillators, CZT, HPG, HgI etc); Hybrid detectors; Instrumentation for synchrotron radiation accelerators

<sup>1</sup>Corresponding author.

---

## Contents

<b>1</b>	<b>Introduction</b>	<b>1</b>
<b>2</b>	<b>Materials and methods</b>	<b>2</b>
2.1	CdTe detector	2
2.2	Timepix chip	2
2.3	Experimental setup at Diamond	3
2.4	X-ray tube experimental setup	3
2.5	Timepix ToT calibration and spectra reconstruction	3
<b>3</b>	<b>Results and discussion</b>	<b>3</b>
3.1	Spectroscopic performance	3
3.2	Imaging performance	5
<b>4</b>	<b>Conclusions</b>	<b>8</b>

---

## 1 Introduction

CdTe, as a  $X$ - and  $\gamma$ -ray detection material, offers much higher detection efficiency in the energy region above  $\sim 30$  keV in comparison to silicon. This opens a broad range of applications for detectors based on CdTe from medical imaging and space sciences to industrial quality control and material studies at synchrotrons. Pixellation of the material creates imaging capabilities while maintaining high stopping power. This, however, significantly complicates the readout of such multi-pixel arrays. In this work the CdTe material was bump-bonded to the 65k pixel Timepix readout ASIC [1]. The chip has several readout modes including single photon counting and energy discrimination mode. The results reported here assess both imaging and spectroscopic performance capabilities for two detectors with 55  $\mu\text{m}$  and 110  $\mu\text{m}$  pixel pitches. There are several alternative developments using similar hybrid pixel detector technology, which are being investigated, PILATUS [2], XPAD [3] and HEXITEC [4]. These all have their own advantages and disadvantages. An interested reader should refer to corresponding publications for details and comparison. The Timepix CdTe assembly offers a portable, small pixel system, capable of 80 frames per second (fps) full frame readout with simultaneous energy discrimination and imaging.

This publication has the following structure: section 2 gives a brief description of the CdTe material and its performance characteristics as well as a summary of key Timepix chip properties and description of the experimental setups at the Diamond Light Source and in the laboratory. Section 3 reports on spectroscopic and imaging performances of the hybrid pixel detector. Finally section 4 summarises the results and outlines future work.

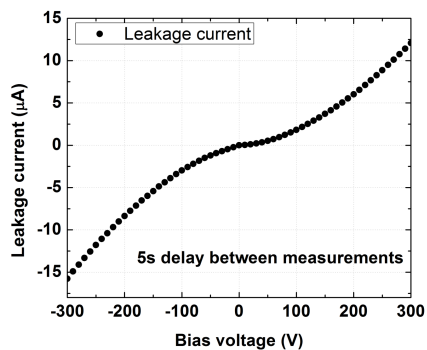


**Figure 1.** Typical current voltage characteristic of  $14 \times 14 \times 1$  mm CdTe detector with Pt contacts bump-bonded to Timepix chip. The current was measured 5 seconds after each voltage was set.

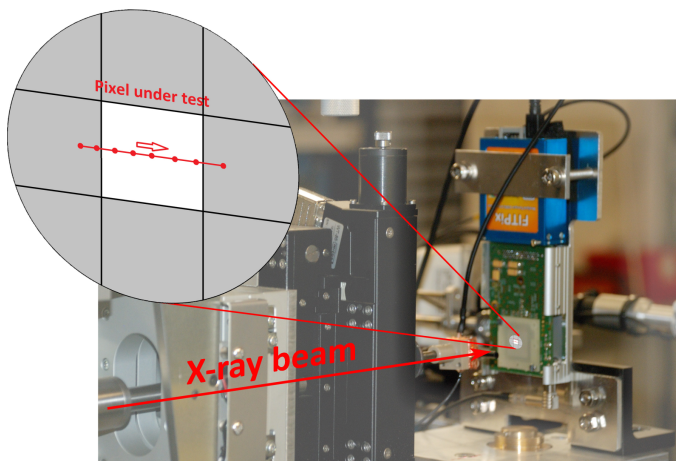


**Figure 2.** Schematic and photo of experimental setup at I15 beam line in Diamond synchrotron. The normally incident monochromatic X-ray beam was scanned across three pixels in ToT mode.

## 2 Materials and methods

### 2.1 CdTe detector

The sensor bump-bonded to the Timepix chip is a 1 mm thick high resistivity p-type *CdTe* material from Acrorad [5]. The die size is  $14 \times 14$  mm matching the size of the readout chip. The pixels and the back side of the detector are Ohmic type Pt contacts. The current-voltage characteristic of the detector already bump-bonded to Timepix is shown in figure 1. The IV establishes quasi-Ohmic behaviour for bias voltages between  $\pm 300$  V. The transport properties of the charge carriers in a similar assembly was investigated in [6]. The values for  $\mu_e \tau_e = (1.9 \pm 0.6) \times 10^{-3} \text{ cm}^2/\text{V}$  and  $\mu_h \tau_h = (0.75 \pm 0.25) \times 10^{-4} \text{ cm}^2/\text{V}$  were obtained. These agree with the other results reported on Acrorad material. The hybridisation of the detector with chip was performed by FMF Freiburg. The details of the process can be found in [7].

### 2.2 Timepix chip

The Timepix chip comprises of  $256 \times 256$  square pixels at  $55 \mu\text{m}$  pitch. Each pixel consists of  $\approx 550$  transistors and has both an analog and a digital part. The analog part contains a charge sensitive amplifier (CSA), which can accept both positive and negative polarities, and a low threshold discriminator with 4-bit trimming. The digital part has a mode control logic unit and a 14-bit counter. The chip can operate in several modes, named *Medipix or counting*, *Time-over-Threshold (ToT)* and *Time-of-Arrival (ToA)*. In counting mode, the value in the counter is incremented every time the CSA output passes the threshold set in the pixel. In ToA mode the time stamp of the particle incident on the detector is recorded, meaning the counter is enabled from the point of interaction until the shutter is closed. In ToT mode the counter starts counting when the CSA output is above the threshold and stops when the charge goes below the threshold. In this mode the number of counts in the pixel is proportional to the energy of the incident radiation.

The chip was attached to the *FITPix USB2.0* interface developed by IEAP in Prague [8]. The assembly can transmit up to 80 *fps* to a PC. *Pixelman* software [9] was used to read out the data and set up the detector. The chip clock signal was set to 48 MHz. The range of bias voltages between  $\pm 500$  V was supplied to the CdTe detector by a *Keithley 237* source-measure unit.

### 2.3 Experimental setup at Diamond

Synchrotron radiation measurements on the  $110 \times 110 \mu\text{m}$  pixel pitch CdTe detector assembly were performed at the Extreme Conditions beam line I15 of the Diamond Light Source [10]. The schematic and photograph of the experiment is shown in figure 2. The detector was placed perpendicular to the incident photon flux and aligned with a laser pointer. A scan of  $220 \mu\text{m}$  across three pixels was performed at energies of 25, 29, 33, 40 and 77 keV from the centre of the leftmost pixel to centre of the rightmost pixel. The step size of  $10 \mu\text{m}$  was chosen to ensure adequate oversampling. The beam size was measured to be  $20 \mu\text{m}$  FWHM at 40 keV. Energy spectra reported in this paper were reconstructed from the beam incident in the middle of the pixel under test.

### 2.4 X-ray tube experimental setup

X-ray spectra and images were acquired on a Thales X-ray tube generator with an Molybdenum anode target. The X-ray tube voltage range is 0–50 kV and the current range 0–50 mA in continuous output. In the experiment it was used with no filtration above the K-edges of the calibration foils at 50 mA. The detector was placed at an angle of 90 degrees to the collimator of the tube. The fluorescence from metal sheets placed 45 degrees to the incident beam and the detector was used to produce quasi-monoenergetic X-rays for energy spectra estimation. For MTF calculations the bremsstrahlung spectrum from a dental X-ray tube was used at 60 kV voltage. No flat field correction of the acquired images was performed. This approach was chosen in order to establish the basic performance of the system without any corrections.

### 2.5 Timepix ToT calibration and spectra reconstruction

Energy calibration of the device was done in accordance with the procedure reported in [11]. Single pixel interactions of low energy X-ray sources (below 60 keV) were recorded and fitted with a non-linear function:

$$ToT = a \times E + b - \frac{c}{t - E} \quad (2.1)$$

The coefficients  $a, b, c$  and  $t$  were extracted and the quadratic equation was resolved against energy. The positive root of the solution was used for  $ToT - to - keV$  data conversion. For  $\gamma$ -sources with energies above  $\sim 100$  keV only the linear part of the equation was employed. The recorded energy spectra was reconstructed by summing the charge converted into keV units in the neighbouring pixels, which passed the threshold.

## 3 Results and discussion

### 3.1 Spectroscopic performance

Spectroscopic performances of both  $55 \mu\text{m}$  and  $110 \mu\text{m}$  pixel assemblies were evaluated in the range of 4–1000 keV by a combination of X-ray/ $\gamma$ -ray sources, target fluorescence from the laboratory X-ray tube and monochromatic synchrotron radiation. The thresholds for both detectors

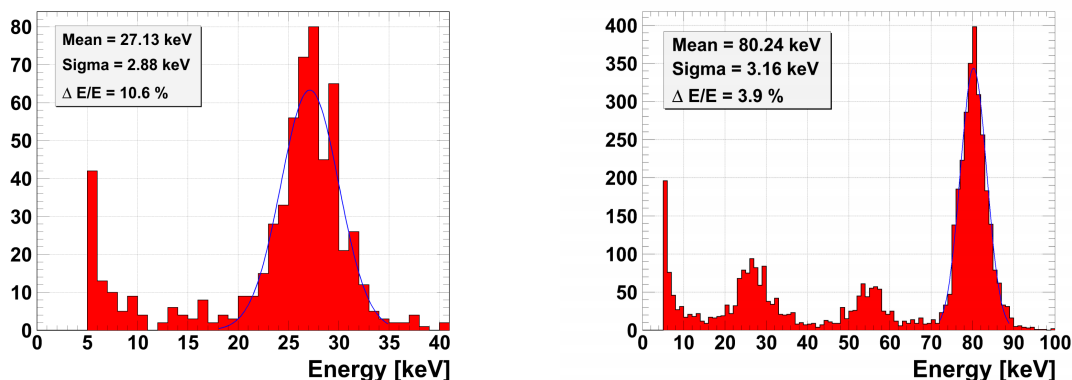


**Figure 3.** Energy spectra recorded with  $110 \times 110 \mu\text{m}$  pixel 1 mm thick CdTe Timepix detector under monochromatic synchrotron radiation (25 keV — left, 77 keV — right).

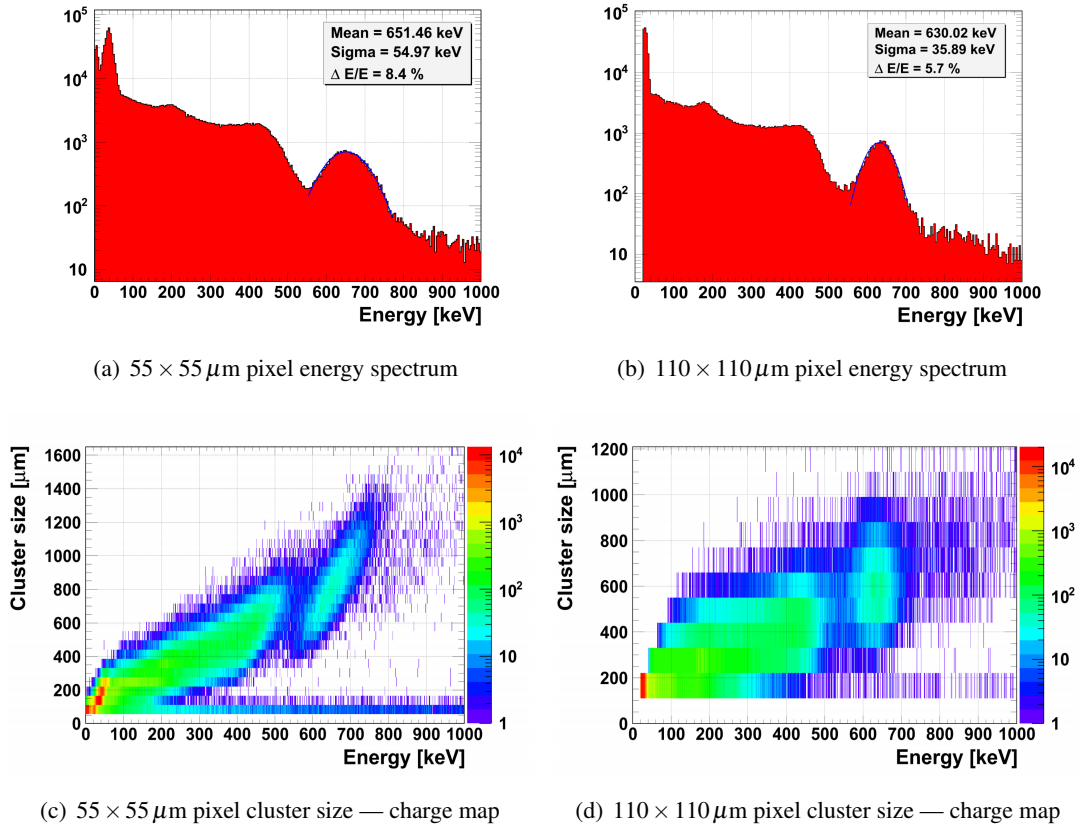
were set globally to  $\sim 5$  keV. The default Timepix clock was set to 48 MHz and the bias voltage to  $-300$  V. The chip was operated in electron collection mode. No spectra correction or enhancement was performed, since the goal of this study was to establish the bottom line performance of the device.

Figure 3 shows spectra recorded by the  $110 \mu\text{m}$  pixel pitch CdTe detector under monochromatic synchrotron radiation at 25 and 77 keV. Energy resolution, calculated as  $R = \Delta E/E$ , was found to be 10.6% and 3.9%, respectively. For 77 keV plot both escape and fluorescence peaks are clearly seen. The detector energy resolution, however, does not allow resolving *Cd* and *Te* characteristic lines.

Figures 4(a) and 4(b) compare the spectra of  $^{137}\text{Cs}$  for both pixel pitch detectors. For the  $55 \mu\text{m}$  pixel the energy resolution of the 662 keV peak is found to be 8.4% compared to 5.7% for the  $110 \mu\text{m}$  pixel. Figures 4(c) and 4(d) show maps of energy spectra dependence on average cluster size. It should be noted that the average cluster size of  $55 \mu\text{m}$  pixel detector is  $800 \mu\text{m}$ , which is  $200 \mu\text{m}$  bigger than for the  $110 \mu\text{m}$  pixel. There is no conclusive explanation for such a difference yet. However, it could be associated with different electrical field profiles near the pixels of different sizes under the same biasing conditions and detector thicknesses. This results in additional diffusion of charge on the smaller pixel.

A combined comparison of the energy resolution between  $55 \mu\text{m}$  and  $110 \mu\text{m}$  pixel pitches on X-ray/ $\gamma$ -ray sources and synchrotron radiation is shown in figure 5. On average the  $110 \mu\text{m}$  pixel detector demonstrates energy resolution better by a factor of two at energies above  $\sim 50$  keV. Rather poor energy resolution was observed on both detectors for X-ray fluorescence and source energies below  $\sim 60$  keV. This could be associated with non-optimised amplifier settings and will be addressed in future studies.

The energy resolution of the  $55 \mu\text{m}$  pixel detector was studied as a function of the bias voltage using the 511 keV peak of a  $^{22}\text{Na}$  source. This can be seen in figure 6. The resolution improves from 13% at  $-100$  V bias voltage to 9% at  $-500$  V. Below  $-100$  V the energy spectrum is significantly distorted, while above  $-500$  V leakage current is too high (above  $-100 \mu\text{A}$ ) to perform measurements.



**Figure 4.**  $^{137}\text{Cs}$  energy spectrum comparison between  $55 \mu\text{m}$  and  $110 \mu\text{m}$  pixel 1 mm thick CdTe detector.

The stability of the detector operation at normal conditions was assessed over period of 8 hours. The bias voltage was set to  $-300 \text{ V}$  and energy spectrum of  $^{22}\text{Na}$  was taken every hour during the day at room temperature. Variation of energy resolution is shown in figure 7. No degradation in the detector performance was observed. Leakage current was also stable at  $9.5 \pm 0.8 \mu\text{A}$ .

### 3.2 Imaging performance

Imaging capabilities of two pixel pitch detectors were evaluated in terms of the modulation transfer function (MTF) with a laboratory X-ray tube. This represents the normalised transfer of contrast through the system at a give spatial frequency, expressed in line pairs per millimetre (lp/mm). A slanted niobium-lead ( $PbNr$ ) edge was placed close to the detector surface at  $\sim 5$  degrees to a sensor row. The detector was exposed to various energies from the X-ray tube. No flat-field correction was performed on the images. An error function was fitted to the edge profile. The Fourier transformation of the derivative normalised to 1 at 0 spatial frequency resulted in the MTF plot.

A comparison between MTFs at various bias voltages for  $55 \mu\text{m}$  pitch detector is presented in figure 8. On the right hand side of the plot there is an illustration of image quality, corresponding to two bias voltages of  $-100$  and  $-500 \text{ V}$ . The best MTF is observed for bias voltages of  $400\text{--}500 \text{ V}$ . Gradual degradation of performance is seen for smaller detector biases. It should be noted that due



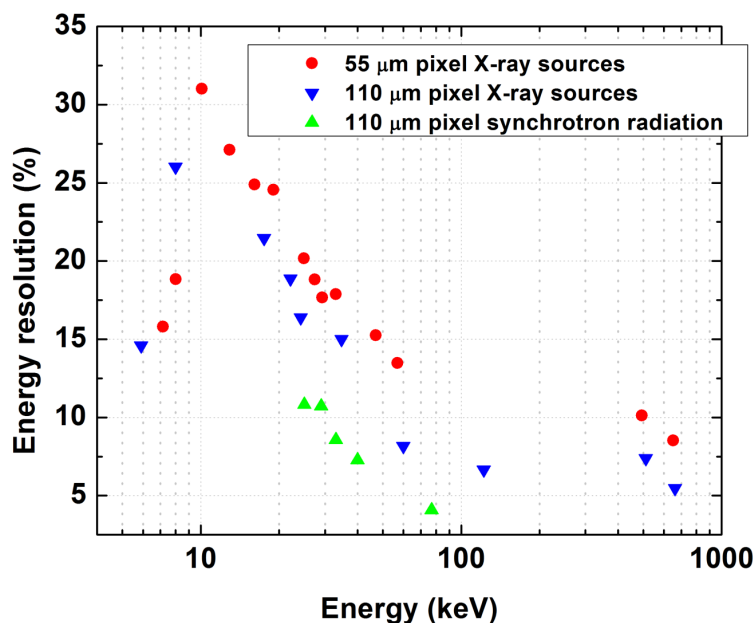


**Figure 5.** Energy resolution comparison between 55  $\mu\text{m}$  and 110  $\mu\text{m}$  pixel detectors recorded at Diamond synchrotron and fluorescence/X-ray sources.

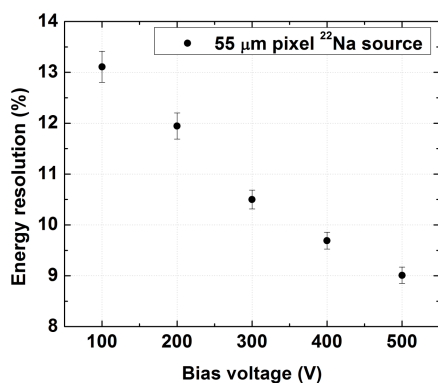


**Figure 6.**  $^{22}\text{Na}$  511 keV peak energy resolution dependence of the 55  $\mu\text{m}$  pixel CdTe detector from bias voltage.

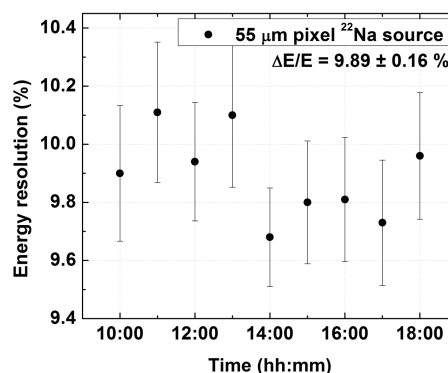


**Figure 7.**  $^{22}\text{Na}$  511 keV peak energy resolution time dependent stability of the 55  $\mu\text{m}$  pixel CdTe detector.

to non-uniformities and defects in the detector material a variation of 10–20% in the MTF taken from various “good” regions in the detector was observed.

The MTF performance was assessed at various X-ray tube cathode voltages. Degradation of  $\sim 10\%$  was observed for X-ray tube energies between 20 and 60 keV, which is mainly associated with the  $PbNr$  being more transparent at higher energies, hence degrading the edge quality. This can be seen in figure 9.

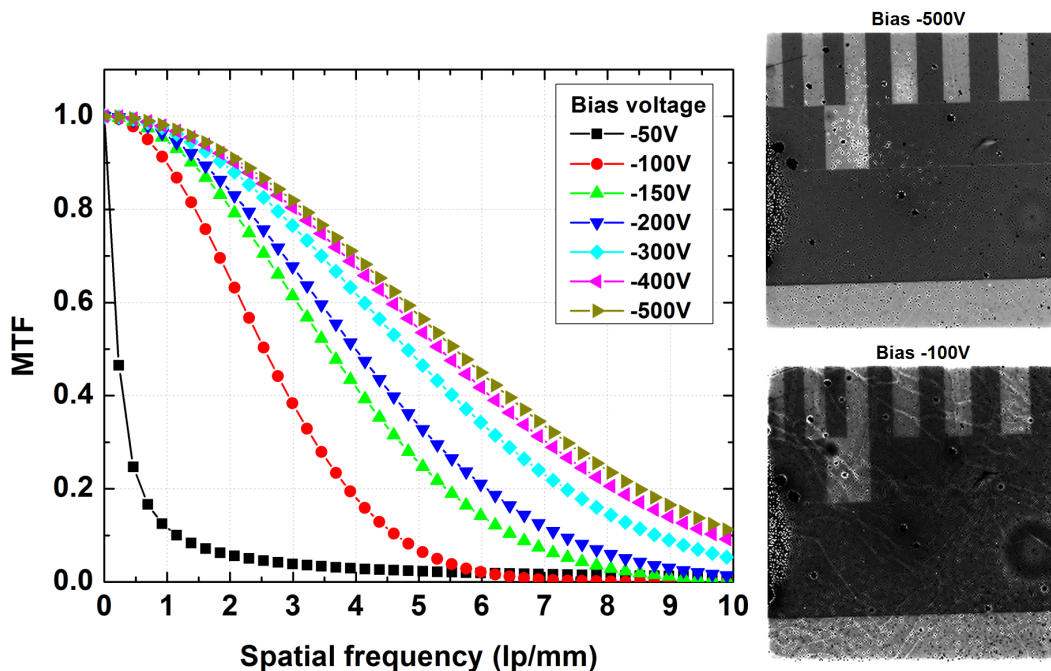


**Figure 8.** MTF dependence on CdTe detector bias voltage recorded with  $55\ \mu\text{m}$  pixel pitch sensor. X-ray tube energy was set to 60 keV. Images to the right demonstrate quality of the image recorded at  $-500\ \text{V}$  and  $-100\ \text{V}$ .

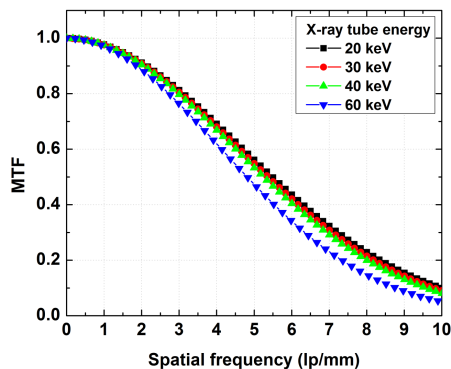


**Figure 9.**  $55\ \mu\text{m}$  pixel detector MTF dependence on X-ray tube voltage. The detector was biased at  $-300\ \text{V}$ , threshold was set to  $\sim 5\ \text{keV}$ .

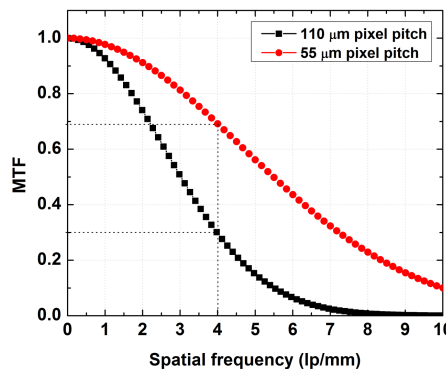


**Figure 10.** MTF comparison between  $55\ \mu\text{m}$  and  $110\ \mu\text{m}$  pixel detectors. Bias voltage applied was  $-300\ \text{V}$ , threshold was set to  $\sim 5\ \text{keV}$ .

A MTF comparison between  $55$  and  $110\ \mu\text{m}$  is shown in figure 10. The X-ray tube was operated at 20 keV, while the detector threshold was set to a noise level of  $\sim 5\ \text{keV}$ . 70% modulation transfer at 4 lp/mm is observed for the  $55\ \mu\text{m}$  pixel compared to 30% for  $110\ \mu\text{m}$ . This is in agreement with expected values for the pixel being double the size.

## 4 Conclusions

Two 1 mm thick CdTe detectors with pixel pitches of 55  $\mu\text{m}$  and 110  $\mu\text{m}$  bump-bonded to Timepix readout ASIC were characterised by means of spectroscopic energy resolutions from a monochromatic X-ray source at Diamond Light Source, various radioactive  $\gamma$ -sources and a laboratory X-ray tube. Imaging performance of the detectors was assessed in terms of modulation transfer at different spatial frequencies.

Energy resolution was found to be systematically better for the 110  $\mu\text{m}$  pixel detector for the energy ranges 10–1000 keV. At energies above  $\sim 100$  keV both detectors demonstrated acceptable spectroscopic performances. For example, the  $^{137}\text{Cs}$  662 keV peak gives  $\Delta E/E = 8.4\%$  for the 55  $\mu\text{m}$  pixel, compared to 5.7% for the 110  $\mu\text{m}$  pixel at  $-300$  V bias voltage. The linear relationship between bias voltage and energy resolution was demonstrated for 511 keV  $\gamma$ -rays. The systematic difference in energy resolution between two pixel pitches is associated with pixel-to-pixel non-uniform response not only in the ASIC but potentially related to the CdTe material itself. This is an issue of further research and will be reported in the near future.

The CdTe detector with 55  $\mu\text{m}$  pitch demonstrates reasonable imaging performance. A 70% contrast at 4 lp/mm was achieved for the 55  $\mu\text{m}$  pixel pitch detector with the 60 kV X-ray tube and 5 keV noise level. No significant degradation in performance was observed for X-ray tube energies of 20–60 keV. The optimal bias voltage for imaging was found to be 400–500 V for 1 mm thick CdTe detector. As expected, around half the contrast transfer (30%) was recorded for 110  $\mu\text{m}$  compared to 55  $\mu\text{m}$  pixel detector at 4 lp/mm.

Significant room for improvement in the assembly performance has been identified. Future work will include energy calibration of each individual pixel, optimisation of pixel preamplifier response and application of various available correction algorithms for enhanced spectra resolving imaging.

## Acknowledgments

The work in this research article has been carried out in the framework of the Medipix collaboration. The authors would like to acknowledge Michael Fiederle from Freiburger Materialforschungszentrum for assistance in bump-bonding Acrorad CdTe material to the Timepix chip.

## References

- [1] X. Llopart et al., *Timepix, a 65k programmable pixel readout chip for arrival time, energy and/or photon counting measurements*, *Nucl. Instr. Meth. A* **581** (2007) 485.
- [2] P. Kraft et al., *Characterization and calibration of PILATUS detectors*, *IEEE Trans. Nucl. Sci.* **56** (2009) 758.
- [3] J.-F. Berar et al., *XPAD3 hybrid pixel detector applications*, *Nucl. Instr. Meth. A* **607** (2009) 233.
- [4] L. Jones et al., *HEXITEC ASIC — a pixellated readout chip for CZT detectors*, *Nucl. Instr. Meth. A* **604** (2009) 34.
- [5] Acrorad, <http://www.acrorad.co.jp/us/index.html>.

- [6] D. Greiffenberg et al., *Energy resolution and transport properties of CdTe-Timepix-Assemblies*, 2011 *JINST* **6** C01058.
- [7] M. Fiederle et al., *Development of flip-chip bonding technology for (Cd,Zn)Te*, *IEEE Trans. Nucl. Science* **51** (2004) 1799.
- [8] V. Kraus et al., *FITPix — fast interface for Timepix pixel detectors*, 2011 *JINST* **6** C01079.
- [9] T. Holy et al., *Data acquisition and processing software package for Medipix2*, *Nucl. Instr. Meth. A* **563** (2006) 254.
- [10] Diamond Light Source Ltd., *Extreme Conditions Beamline I15*, <http://www.diamond.ac.uk/Home/Beamlines/I15.html>.
- [11] J. Jakubek et al., *Pixel detectors for imaging with heavy charged particles*, *Nucl. Instr. Meth. A* **591** (2008) 155.